

Rigidity of fragile matter: a gauge theoretic perspective

Bulbul Chakraborty^{1,*}

¹Martin Fisher School of Physics, Brandeis University, Waltham, MA 02454

Abstract. The process of jamming creates fragile matter, whose rheology is distinct from solids or liquids. The solidity of fragile matter emerges from the applied stress itself. Despite their disordered, fluid-like structure, they can exhibit elastic behavior under small perturbations. The rigidity of these solids emerge from internally organized contact networks created by external forces such as gravity or confinement. Unlike traditional elastic solids, these fragile solids do not possess a stress-free reference structure. This poses challenges for classical elasticity, whose formulation relies on strain, relative to a stress-free configuration. This has, for decades, motivated the search for a stress-only elasticity framework. Recent advances have provided a new perspective based on a gauge theoretic framework defined by a generalization of the familiar Gauss's law of electromagnetism. For fragile, granular solids, the Gauss's law represents the constraints of mechanical equilibrium. Elasticity emerges as a "dielectric" response to external stresses: internal, bound force dipoles, screen external forces. This paper presents a short review of this theoretical framework.

1 Introduction

In a 1998 paper [1], entitled "Jamming, Force Chains, and Fragile Matter", the authors state that fragile matter can statically support shear stresses "but only by virtue of a self-organized internal structure, whose mechanical properties have evolved to support the load itself". Therefore, it has an elastic response only to compatible loads. This behavior does not fit within the paradigm of classical elasticity theory, for which, strain about a given reference state is foundational, and stress is a *derived* quantity [2]. The quest for a stress-only formulation of the elasticity of jammed, granular solids can be traced back to the 1998 paper [1]. The rationale behind this notion, and the theoretical and experimental efforts to establish a comprehensive theory based on it, has been elaborated on and summarized in lecture notes [3] and review articles [4]. The development of a gauge-theoretic framework, which extended classical electromagnetism to fields that were symmetric tensors and charges that are vectors [5], have now allowed us to construct a rigorous and comprehensive continuum theory of stress-only elasticity [6–9].

Jammed solids, composed of non-Brownian particles with purely repulsive interactions, acquire rigidity when an externally applied stress exceeds a critical threshold [10–12]. This mechanism defines the jamming transition, a unifying concept of rigidity in disordered materials such as foams, emulsions, and granular media [11–15]. Jammed solids, therefore, belong to a class of solids where the mechanical response *emerges* from the frozen-in internal stresses, or prestress [16]. Since the solidity of jammed solids emerges from the imposed stress itself, and the rigid *structure* is created in response to stress, there is no unique

zero-stress *reference* solid network [1, 3]. It is the mechanical response to *additional* stress that determines whether the system is rigid or not. Under these circumstances, one may conclude that both of the fundamental ideas of the theory of crystalline elasticity—the existence of a strain tensor defined with reference to a unique stress-free spontaneously broken-symmetry configuration, and a free energy relating stress to strain—need to be re-visited and may have to be abandoned [3, 17].

Curiously however, the mechanical properties of jammed solids bear many similarities to crystalline elasticity [17–21]. For example, the response of a granular pile [17, 20] or that of frictionless jammed packings [21, 22] to point forces, can be described in terms of effective elastic moduli and elastic Green's functions. However, these *elastic* moduli do not necessarily satisfy the usual symmetry requirements [17] and depend on preparation protocols [17, 21]. Stress-stress correlations also exhibit power-law decays as expected for elastic media [18, 19]. This poses a puzzle since, *e.g.* the theory of crystalline elasticity is based on the existence of a periodic reference structure – emerging from spontaneously broken translation symmetry in crystals – which then defines a strain field via systematic coarse-graining [2, 23]. While the stress field is well defined in jammed solids, the lack of a unique reference configuration makes the definition of the strain field and the associated free energy much less apparent.

This puzzle and associated issues gave birth to the quest for a stress-only continuum theory of the elasticity of jammed solids [3]. In frictionless systems, jammed solids are the minima in a complex energy landscape. The non-cohesive nature of granular interactions implies that the breaking and forming of contacts play an essential

*e-mail: bulbul@brandeis.edu

role in the mechanical response of these jammed solids to external forces rendering the response inherently anharmonic [24]. This has also led to a concentrated effort to understand plasticity in amorphous solids [25–28] based on notions of non-affine displacements. In frictionless jammed solids, there is a potential that defines the relationship between displacements and forces [21], and one can attempt to include contact-breaking into this framework to understand the full mechanical response of these solids. In frictional jammed solids, the notion of strong and weak force networks [29] has played a major role in understanding the mechanical response. A different perspective, based on a coarse-graining of the grain level elastic deformations [30] has led to a continuum or hydrodynamic theory of granular elasticity. The virtual displacement ansatz [31] also addresses the challenge of integrating micromechanics into a continuum, field theoretic description. In this context, there is also a rich and long history of elastoplastic models [32]. In the language of elasticity, the challenge that the granular community has been addressing is to construct a framework that can produce a constitutive relation relating stress to displacements.

This paper reviews a recently developed theoretical framework [6, 7] that eliminates the the notion of displacements and a constitutive relation relating these to stress, and constructs a stress-only, continuum theory [3] of the mechanical response of granular solids.

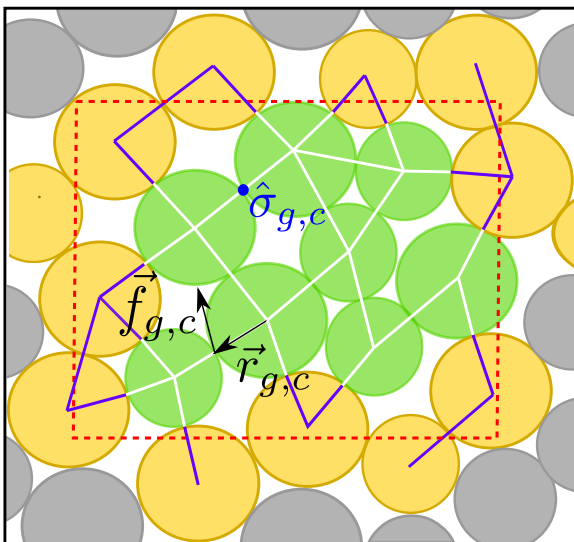


Figure 1. A schematic depiction of a packing of grains (discs) in two dimensions (2D) [6] (Copyright (2022) by the American Physical Society): Each grain is in mechanical equilibrium and satisfies the microscopic constraints of force and torque balance that leads to a non-trivial contact network. A large packing consists of many local structures, which can be coarse grained (say over the red box with volume Ω), to produce a continuous stress field. Grains with all contacts in Ω , are identified as bulk grains (colored green), whereas grains with a partial overlap with Ω , are identified as boundary grains (colored yellow). Each contact has two contributions to the coarse grained stress tensor $\sigma(\mathbf{r})$. The white (violet) contact links contribute to the (anti)-symmetric part of the total stress tensor.

At the heart of the mechanical response of jammed, granular solids is the athermal, non-Brownian, nature of these assemblies consisting of configurations at mechanical equilibrium implemented locally: each grain is in a state of force and torque balance as shown in Fig. 1. These local constraints lead to a non-trivial contact network that is in static force and torque balance [33]. The emergence of such disordered structures from local constraints of mechanical equilibrium is challenging to incorporate in any continuum theory. In the naive continuum limit, force and torque balance do not provide enough equations to uniquely determine the stress distribution [3]. Stated differently, since it is not possible to define a strain field with respect to a unique stress-free state, the well-known compatibility relations of linear elasticity theory are missing, and the linear response coefficients of crystalline elasticity stemming from proportionality between stress and strain—the so called elastic moduli, are not well defined [2].

2 Stress-only Elasticity:VCTG

A new framework has been put forward [6] to supply the *missing compatibility equations* to obtain the much cherished *stress-only* description of granular elasticity. Central to this framework is a gauge theoretic structure that arises from— (1) the lack of a well-defined and unique zero-stress reference configuration and (2) the local mechanical equilibrium of each grain in an athermal solid. The latter serves as a generalized “Gauss’s law” for the stress tensor, which maps on to a *tensor electric field* of the so called *vector charge theory* (VCT) [34] of *tensor electromagnetism*. Just as in classical electromagnetism, VCT is described by Maxwell’s equations involving electric and magnetic fields, both of which are symmetric tensors. In mapping the *electrostatics* of VCT to the a theory of the mechanical response of granular solids, the vector charges become the free or unbound forces on grains, and the electric field maps to the stress. The Gauss’s law of VCT generates *two* conserved quantities, the vector charge, and the associated charge-angular-momentum. In the mapping to granular solids, these translate to force and torque balance [6, 7]. Determining stress transmission in a jammed granular solid then maps to the problem of solving electrostatics in the presence of *dielectric screening* in the VCT. This stress-only framework, dubbed as VCTG, is completely devoid of any reliance on a reference structure. The prestress represented by the contact force-moments, appears as the analog of the familiar polarization field present in a dielectric in standard electrostatics. In contrast to standard electrostatics, however, this polarization field is a second rank tensor [6]. This gauge-theoretic structure also accommodates a Debye-type screening defined by a finite screening length [9, 28, 35–37].

Following the framework of standard electrostatics of a dielectric medium [38], we divide charges (forces) into

$$f_i = f_i^{\text{ext}} + f_i^{\text{bound}}, \quad (1)$$

such that the Gauss’s law is now written as

$$\partial_i E_{ij} = f_i^{\text{ext}} + f_i^{\text{bound}}, \quad (2)$$

where, \mathbf{f}^{ext} are external forces such as gravity, and $\mathbf{f}^{\text{bound}}$, are the bound, contact forces, that appear in the polarizable medium in response to the external forces. Note that we use index notation to indicate the cartesian components of vectors and tensors, and use bold symbols denote these structures themselves.

The multipole expansion within VCTG leads to [6]:

$$\mathbf{f}_i^{\text{bound}} = -\partial_j \mathcal{P}_{ij}(\mathbf{r}), \quad (3)$$

where $\mathcal{P}_{ij}(\mathbf{r})$, the analog of the dipole moment density, is the prestress field created by the contact forces. This is the sense in which jammed granular solids are polarizable. External forces, such as gravity, create a contact network of grains, which can support the external stress. This process is akin to creating dipole fields in a dielectric: grains pushed together by the external force, deform, even if infinitesimally, creating contact forces, $\mathbf{f}^{\text{bound}}$. Eq. (2) can now be re-written as

$$\partial_i \sigma_{ij} = f_j^{\text{ext}}, \quad \text{with} \quad \sigma_{ij} = E_{ij} + \mathcal{P}_{ij} \quad (4)$$

where σ_{ij} , the stress tensor, appears as the analog of a *screened tensor electric field*, the analog of the electrostatic displacement field. Modeling granular solids as a linear dielectric, the polarizability is proportional to the unscreened stress field,

$$\mathcal{P}_{ij} = \chi_{ijkl} E_{kl}, \quad (5)$$

where χ is the polarizability tensor. Note that the assumption of a linear relation between $\hat{\mathcal{P}}$ and \hat{E} is not equivalent to a linear response in displacements, and a Hessian framework. In particular, the microscopic nonlinearities emerging from contact breaking and formation [24] are included in the continuum prestress field, $\hat{\mathcal{P}}$.

Using Eq. (5), the stress tensor can be re-written as

$$\sigma_{ij} = (\delta_{ijkl} + \chi_{ijkl}) E_{kl} \equiv (\Lambda^{-1})_{ijkl} E_{kl}. \quad (6)$$

with Λ^{-1} being a rank-4 dielectric tensor. Since E_{ij} is symmetric, χ_{ijkl} is given by a linear combination of symmetric and anti-symmetric parts in the indices i and j as

$$\chi_{ijkl}^A = \chi_{ijkl} - \chi_{jikl}, \quad \chi_{ijkl}^S = \chi_{ijkl} + \chi_{jikl}. \quad (7)$$

This leads to symmetric and anti-symmetric contributions to \mathcal{P}_{ij} :

$$\mathcal{P}_{ij}^A = \chi_{ijkl}^A E_{kl}, \quad \mathcal{P}_{ij}^S = \chi_{ijkl}^S E_{kl}. \quad (8)$$

These antisymmetric contributions imply that, for frictional grains, a boundary force can lead to a finite antisymmetric polarisation, *i.e.* the boundary torque, which may lead to shearing of the boundary layer [39, 40]. Putting these together, the field equations of VCTG are given by [6] Eqs. (4) and (6) along with,

$$E_{ij} = \frac{1}{2}(\partial_i \varphi_j + \partial_j \varphi_i) \implies \epsilon_{iab} \epsilon_{jcd} \partial_a \partial_c E_{bd} = 0. \quad (9)$$

The above equation, which represents the compatibility condition, appears in VCTG as the *static limit* of Faraday's

equation in VCT [6]. Comparing the structure of the above *gauge theoretic framework* with that of crystalline elasticity [2], shows a clear correspondence between VCTG and the theory of elasticity, captured by the equations:

$$\begin{aligned} \partial_i \sigma_{ij} &= f_j^{\text{external}}, \\ E_{ij} &= \frac{1}{2}(\partial_i \varphi_j + \partial_j \varphi_i) \implies \epsilon_{iab} \epsilon_{jcd} \partial_a \partial_c E_{bd} = 0, \\ \sigma_{ij} &= (\delta_{ijkl} + \chi_{ijkl}) E_{kl} \equiv \Lambda_{ijkl}^{-1} E_{kl} \end{aligned} \quad (10)$$

if we make the following map:

$$\begin{aligned} \hat{E} &\leftrightarrow \hat{\gamma} \quad \text{the strain tensor,} \\ \Lambda_{ijkl}^{-1} &\leftrightarrow K_{ijkl} \quad \text{the elastic modulus tensor.} \end{aligned} \quad (11)$$

2.1 Distinctions between VCTG and Classical Elasticity

Eqs. 10 and 11 appear to have the same structure as classical elasticity. So, why is this a stress-only formulation and what are the essential differences between VCTG and classical elasticity? One set of important distinctions relate to the mapping between \hat{E} and $\hat{\gamma}$. The mapping in Eq. 11 involves dimension-full constants since \hat{E} is a stress, not strain. The physical interpretation of \hat{E} is that it would be the stress created inside a solid due to externally imposed stresses, such as gravity, if the grains were not allowed to deform at all and create contact forces. It is *not related* to displacements from any ideal reference configuration or metric [35]. The compatibility relation (second equation in Eq. 10) is a consequence of the Faraday's law in VCTG [6]:

$$\epsilon_{iab} \epsilon_{jcd} \partial_a \partial_c E_{bd} = -\partial_i B_{ij} - \tilde{J}_{ij} \quad (12)$$

where, \hat{B} is the analog of the magnetic field. This field is sourced by the momenta, π of grains, which are the analogs of magnetic charges in VCTG:

$$\partial_i B_{ij} = \pi_j. \quad (13)$$

In the static limit, the ‘‘magnetic charge’’ is zero. The other source of generation of \hat{B} is the VCTG Ampere's law, which involves time derivative of \hat{E} [6], which also vanishes in the static limit. Therefore, both sources of incompatibility of \hat{E} are zero, leading to the gauge-potential formulation in terms of the field φ . The implications is that unlike strain fields which become incompatible in the presence of *static* defects [35, 41], the unscreened stress, \hat{E} , can only become incompatible in the presence of dynamics. The other striking result from VCTG is that the *screened stress*, $\hat{\sigma}$, can become *incompatible*. Just as in the theory of dielectric electrostatics, the screened field can be incompatible. The source of this incompatibility, is the polarization stress, \mathcal{P}_{ij} , which emerges from the ‘‘bound’’ forces, the contact forces between grains. Further, we note that because of the antisymmetric contribution to \mathcal{P}_{ij} , the stress tensor is not necessarily symmetric but can have an antisymmetric boundary contribution. Indeed, in frictional granular materials, the possibility of an anti-symmetric contribution to the stress tensor has been widely recognized and is often addressed via the theoretical framework

of Cosserat elasticity [42]. The VCTG formulation clearly identifies the anti-symmetric boundary contribution to $\hat{\sigma}$ as arising from the dipole moment tensor \hat{P} .

VCTG, therefore, addresses both the lack of a canonical definition of a strain tensor $\hat{\gamma}$, arising from the fact that there is no unique reference state about which we can define displacement fields \mathbf{u} , and the lack of a canonical constitutive relation. The relation between stress and strain in classical linear elasticity theory is via the elastic modulus tensor, \hat{K} . In VCTG, this is replaced by the polarizability tensor (Eq. 5 relating \hat{P} to \hat{E} , and $\hat{\chi}$, can depend on the jamming protocol [7]).

Another distinction with classical elasticity theory, is the framework itself. In classical elasticity theory, strain, derived from displacements leads to an energy (or free energy) cost [2], and stress is derived from taking a derivative of the free energy with respect to strain. So, energy conservation and momentum conservation are the two fundamental principles. In VCTG, the “conserved” quantities are “charge” (force balance) and “charge angular momentum” (torque balance).

VCTG successfully predicts long-range anisotropic stress correlations that decay as a power law, $1/r^d$, in d dimensions [43–46], confirmed in 2D/3D via numerical models and experiments on frictional granular systems. This gauge theory identifies pinch-point singularities in Fourier-space correlations (explicit expressions are given in the next section). This is a hallmark of stress correlations in granular systems [46–49]. The implications of these pinch-point singularities on the real-space stress field, $\sigma_{ij}(\mathbf{r})$, is even more dramatic and provides a natural explanation for “force-chains” [7]. To give a simple example, the correlations of σ_{xx} decay as a power law in the x direction, however, in the transverse directions, the correlations become negative over a microscopic, grain length scale, and then decay as a power law, approaching zero from below. This is reflected in the differences between force network images depicted in [50] for isotropic compression and shear. In the former, there are no clear chains since no particular stress component dominates. In contrast, under shear, the stress component in the compressive direction dominates and they form chains along his direction (positively correlated). The chains represent the fact that in the transverse direction the correlations become negative. This origin of the visual appearance of force chains is also evident in [51], where the “chains” appear in different directions in the *same* configuration, when colored by different components of the stress.

The VCTG predictions have been tested in granular solids at high pressures and in gels near the rigidity transition, as well as near-crystalline systems [6–8, 52–54]. The following sections provide a summary of (i) tests of VCTG in granular solids, (ii) applications of VCTG to analyze stress correlations in gels, and introduces some new work on exploring the relationship between the potential φ , and measured displacement fields, and the nature of plasticity and nonlinear screening close to the unjamming transition.

3 Correlations and Response in Granular Solids

VCTG is a field theory that predicts response and correlation functions, and it provides a rigorous basis for the emergence of stress heterogeneities such as “force-chains” [6–8]. It has to be emphasized that VCTG is a disorder-averaged theory, *i.e.*, it predicts the behavior of an ensemble of jammed states subjected to the same set of external stresses [6]. In other words it provides the correlations and response in a Edwards stress ensemble [56]. The explicit forms for these ensemble-averaged stress-stress correlations, in q -space,

$$C_{ijkl}(\mathbf{q}) \equiv \langle \langle \Delta \tilde{\sigma}_i(\mathbf{q}) \Delta \tilde{\sigma}_j(-\mathbf{q}) \rangle \rangle \quad (14)$$

corresponding to an isotropic elastic modulus tensor, K characterized by two Lamé parameters, are given below [6]. In 2D, using polar coordinates, $q_x = q \cos(\theta)$, $q_y = q \sin(\theta)$, these are:

$$\begin{aligned} C_{xxxx}(q, \theta) &= 4K_{2D} \sin^4 \theta \\ C_{yyyy}(q, \theta) &= 4K_{2D} \cos^4 \theta \\ C_{xyxy}(q, \theta) &= 4K_{2D} \sin^2 \theta \cos^2 \theta \\ C_{xxxy}(q, \theta) &= 4K_{2D} (-\sin^3 \theta \cos \theta) \\ C_{xxyy}(q, \theta) &= 4K_{2D} \sin^2 \theta \cos^2 \theta \\ C_{xyyy}(q, \theta) &= 4K_{2D} (-\sin \theta \cos^3 \theta) \end{aligned} \quad (15)$$

with $K_{2D} = \mu \left(\frac{\lambda + \mu}{\lambda + 2\mu} \right) = \frac{\mu}{2(1-\nu)}$, and $\nu = \frac{\lambda}{2(\lambda + \mu)}$ is the Poisson’s ratio. The explicit forms of the three dimensional stress-stress correlations, using polar coordinates, $\{q, \theta, \Phi\}$, are given by,

$$\begin{aligned} C_{xxxx}(q, \theta, \Phi) &= 4(\mathcal{K}_1 + \mathcal{K}_2) \left[\sin^2 \theta \sin^2 \Phi + \cos^2 \theta \right]^2 \\ C_{yyyy}(q, \theta, \Phi) &= 4(\mathcal{K}_1 + \mathcal{K}_2) \left[\sin^2 \theta \cos^2 \Phi + \cos^2 \theta \right]^2 \\ C_{zzzz}(q, \theta, \Phi) &= 4(\mathcal{K}_1 + \mathcal{K}_2) \left[\sin^4 \theta \right] \end{aligned} \quad (16)$$

$$\begin{aligned} C_{xxyy}(q, \theta, \Phi) &= \left[(\mathcal{K}_1 + \mathcal{K}_2) \sin^4 \theta \sin^2 2\Phi + 2\mathcal{K}_2 \cos^2 \theta \right] \\ C_{xxzz}(q, \theta, \Phi) &= \left[(\mathcal{K}_1 + \mathcal{K}_2) \sin^2 2\theta \cos^2 \Phi + 2\mathcal{K}_2 \sin^2 \theta \sin^2 \Phi \right] \\ C_{yyzz}(q, \theta, \Phi) &= \left[(\mathcal{K}_1 + \mathcal{K}_2) \sin^2 2\theta \sin^2 \Phi + 2\mathcal{K}_2 \sin^2 \theta \cos^2 \Phi \right] \end{aligned} \quad (17)$$

$$\begin{aligned} C_{xyxy}(q, \theta, \Phi) &= (\mathcal{K}_1 + \mathcal{K}_2) \sin^4 \theta \sin^2 2\Phi + \\ &\quad (2\mathcal{K}_1 + \mathcal{K}_2) \cos^2 \theta \\ C_{xzxz}(q, \theta, \Phi) &= (2\mathcal{K}_1 + \mathcal{K}_2) \sin^4 \theta \sin^2 \Phi + \sin^2 \theta \cos^2 \theta \\ &\quad \times \left((2\mathcal{K}_1 + 3\mathcal{K}_2) \cos^2 \Phi + (2\mathcal{K}_1 + \mathcal{K}_2) \right) \\ C_{yzyz}(q, \theta, \Phi) &= (2\mathcal{K}_1 + \mathcal{K}_2) \sin^4 \theta \cos^2 \Phi + \sin^2 \theta \cos^2 \theta \\ &\quad \times \left((2\mathcal{K}_1 + 3\mathcal{K}_2) \sin^2 \Phi + (2\mathcal{K}_1 + \mathcal{K}_2) \right) \end{aligned} \quad (18)$$

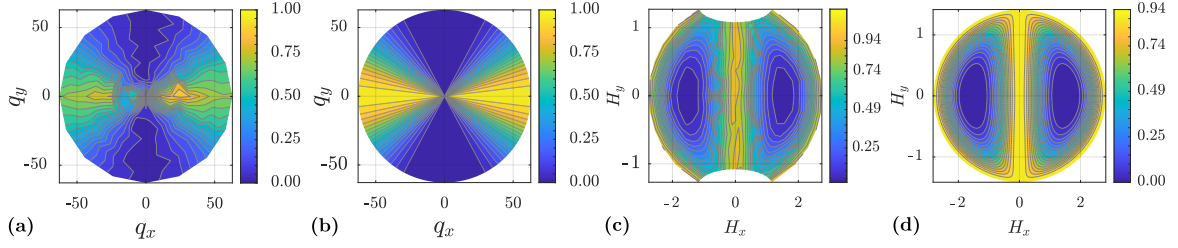


Figure 2. Comparison of the correlation functions obtained from numerical simulations [6](Copyright (2022) by the American Physical Society) with the theoretical predictions, in 3D. The comparisons are done on a system of 27000 grains at packing fraction $\phi = 0.69$. Panels (a) and (b) show respectively, the numerical and theoretical forms for a slice of the correlation function $C_{yyyy}(\mathbf{q})$ on the XY-plane ($\theta = \pi/2$). The pinch-point structure at $|\mathbf{q}| = 0$ is clearly visible. Panels (c) and (d) show the numerical and theoretical results for $C_{yyyy}(\mathbf{q})$ respectively. The results are presented in the Hammer projection [55] coordinates H_x and H_y . The missing regions in the numerics is due to difficulties in sampling around $\theta = 0$ and $\theta = \pi$.

$$\begin{aligned}
 C_{xxxy}(q, \theta, \Phi) &= -4(\mathcal{K}_1 + \mathcal{K}_2) \left(\sin^2 \theta \sin \Phi \cos \Phi \right. \\
 &\quad \left. \left[\sin^2 \theta \sin^2 \Phi + \cos^2 \theta \right] \right) \\
 C_{xxxz}(q, \theta, \Phi) &= -4(\mathcal{K}_1 + \mathcal{K}_2) \left(\sin \theta \cos \theta \cos \Phi \right. \\
 &\quad \left. \left[\sin^2 \theta \sin^2 \Phi + \cos^2 \theta \right] \right) \\
 C_{yyyyx}(q, \theta, \Phi) &= -4(\mathcal{K}_1 + \mathcal{K}_2) \left(\sin^2 \theta \sin \Phi \cos \Phi \right. \\
 &\quad \left. \left[\sin^2 \theta \cos^2 \Phi + \cos^2 \theta \right] \right) \\
 C_{yyyxz}(q, \theta, \Phi) &= -4(\mathcal{K}_1 + \mathcal{K}_2) \left(\sin \theta \cos \theta \sin \Phi \right. \\
 &\quad \left. \left[\sin^2 \theta \cos^2 \Phi + \cos^2 \theta \right] \right) \\
 C_{zzzx}(q, \theta, \Phi) &= -4(\mathcal{K}_1 + \mathcal{K}_2) \sin^3 \theta \cos \theta \cos \Phi \\
 C_{zzzy}(q, \theta, \Phi) &= -4(\mathcal{K}_1 + \mathcal{K}_2) \sin^3 \theta \cos \theta \sin \Phi \quad (19)
 \end{aligned}$$

$$\begin{aligned}
 C_{xxyz}(q, \theta, \Phi) &= \sin 2\theta \sin \Phi \left[\mathcal{K}_2 - 2(\mathcal{K}_1 + \mathcal{K}_2) \cos^2 \Phi \sin^2 \theta \right] \\
 C_{yyxz}(q, \theta, \Phi) &= \sin 2\theta \cos \Phi \left[\mathcal{K}_2 - 2(\mathcal{K}_1 + \mathcal{K}_2) \sin^2 \Phi \sin^2 \theta \right] \\
 C_{zzxy}(q, \theta, \Phi) &= \sin^2 \theta \sin 2\Phi \left[(\mathcal{K}_1 + \mathcal{K}_2) \cos 2\theta + \mathcal{K}_1 \right] \quad (20)
 \end{aligned}$$

$$\begin{aligned}
 C_{xxyz}(q, \theta, \Phi) &= -\sin \theta \cos \theta \sin \Phi \\
 &\quad \times \left[(\mathcal{K}_1 + \mathcal{K}_2) (\cos 2\theta - 2 \sin^2 \theta \cos 2\Phi) + \mathcal{K}_1 \right] \\
 C_{xyyz}(q, \theta, \Phi) &= -\sin \theta \cos \theta \sin \Phi \\
 &\quad \times \left[(\mathcal{K}_1 + \mathcal{K}_2) (\cos 2\theta + 2 \sin^2 \theta \cos 2\Phi) + \mathcal{K}_1 \right] \\
 C_{xzyz}(q, \theta, \Phi) &= \sin^2 \theta \sin 2\Phi \left[(\mathcal{K}_1 + \mathcal{K}_2) \cos 2\theta + \frac{\mathcal{K}_2}{2} \right] \quad (21)
 \end{aligned}$$

where $\mathcal{K}_1 = \mu \left(\frac{\mu}{\lambda + 2\mu} \right)$, $\mathcal{K}_2 = \mu \left(\frac{\lambda}{\lambda + 2\mu} \right)$. From these, we can obtain λ and μ as $\mu = \frac{\mathcal{K}_2}{2\mathcal{K}_1 + \mathcal{K}_2}$, $\lambda = \frac{\mathcal{K}_2}{\mathcal{K}_1} (2\mathcal{K}_1 + \mathcal{K}_2)$. The 3D correlations have been grouped according to their correspondence in the Voigt notation [6], in which, the symmetry of the stress tensor is used explicitly to express it as a column vector with components $\{\sigma_{xx}, \sigma_{yy}, \sigma_{zz}, \sigma_{xy}, \sigma_{xz}, \sigma_{yz}\}$. Denoting these as $\{\sigma_1, \sigma_2, \sigma_3, \sigma_4, \sigma_5, \sigma_6\}$, the first group represents self-correlations elements 1 – 3, the second group to cross-correlations between these components, and so on.

An important feature of these correlations is their independence of $q \equiv |\mathbf{q}|$. They are only dependent on the angular variables θ , and ϕ . Hence, the correlations display singular behavior as one approaches $q \rightarrow 0$ producing a pinch-point at $q = 0$ [6, 7]. This is clearly seen in Fig. 2. Such pinch-point behaviour has previously been identified in the literature [26, 51, 57–59] as a salient feature of the stress correlations of granular systems. These expressions can also be obtained via symmetry arguments if the pressure correlations are known or measured [45]. In contrast, VCTG makes predictions that depend only on the coupling constants of the theory, the elastic moduli. VCTG makes no predictions about these elastic moduli, they enter as parameters of the theory in the guise of the polarizability of the media. As such, they explicitly depend on the details of the underlying contact network. The utility of the VCTG predictions is that the elastic moduli can be inferred from measurements of stress-response and correlation functions. It would be desirable to infer elastic moduli in terms of more readily measurable quantities such as grain displacements in response to external forces. Our recent work, discussed briefly in Section 5, provides such a pathway.

The current formulation shows that striking features of stress response in granular solids emerge purely from the requirement of gauge invariance, and even more importantly, VCTG allows us to compute the explicit angular distributions for any form of the elastic modulus tensor \hat{K} , and then obtain these emergent moduli by fitting numerical or experimental data to these predicted forms. The moduli are emergent because they are determined by the properties of the force-bearing contact network, which in turn is *created* by the externally imposed stresses. We have demonstrated the remarkable success of this approach in frictionless jammed solids in both 2D and 3D [6], and in experiments on frictional packings in 2D [7].

VCTG also successfully predicts the response of jammed granular packings to perturbing forces, deep in the jammed region [6], as illustrated in Fig. 3. This figure shows the stress response of a 2D, frictionless, isotropically jammed packing to an external force distribution:

$$\mathbf{f}^p(x, y) = \left(\frac{1}{L} \delta(y) - \frac{1}{\pi r_0^2} \Theta(r_0^2 - x^2 - (y - a)^2) \right) F \hat{y},$$

where L is the size of the simulation box, a is the y-position of the external force, $r_0 \ll L$ is the size of the coarse-graining region, over which the grains experience the perturbing force with a total magnitude $F \approx 10$ (compared with the average contact force ≈ 0.1), and a compensating line of forces is imposed at $y = 0$ [6]. Recent work on exploring this response for the emergence of a non-trivial length scale will be discussed briefly at the end of the paper.

4 Stress Correlations in Gels

Gels are a class of non-equilibrium, particulate solids that are distinct from dry granular solids in that (a) they have attractive forces, and (b) the protocol for their creation depends on temperature: quenches to force balanced states are from well-equilibrated states.

The rigidity of a broad range of amorphous solids, including soft particulate gels and granular solids, has been widely analyzed using the framework of rigidity percolation theory [60–64]. This framework is based on the idea that locally rigid structures (due to mechanical constraints such as contacts, chemical bonds or steric repulsion) percolate through the material. This concept has been pivotal in clarifying the role played by microscopic properties in giving rise to macroscopic mechanical response, that is, which parts of the microstructure, self-assembled during the solidification process, may satisfy, and how, the conditions corresponding to mechanical equilibrium and Maxwell’s criterion for rigidity.

Rigidity percolation predicts the properties of rigid clusters in *discrete* stress-bearing network. As discussed earlier, VCTG is a continuum stress-only theory of elasticity where the properties of the network enter through the prestress, determining emergent elastic moduli. Establishing connections between the rigid-cluster properties of networks and the VCTG is, therefore, desirable in order to obtain better understanding of this micro-macro connection.

Although rigidity percolation has been applied to frictional granular solids [61], the theoretical basis is not as well-founded as it is for gels with central-force interactions. In recent work [52], we have used the predictive framework of VCTG to interpret the stress-stress correlations measured in such model colloidal gels through 2D computer simulations and established connections between the rigidity percolation framework and the VCTG framework in inferring the onset of rigidity. From the stress correlations, we have also estimated the emergent elastic moduli of gels as predicted by VCTG. This has revealed correlations between normal stresses and mechanical strength in this class of materials. We have also extended the VCTG theory to include the possibility of a Debye-like screening [9, 52], and applied it to 2D gels to look for an emergent length-scale at the rigid to floppy transition.

Fig. 4 illustrates the sensitivity of the pinchpoint singularity in stress-stress correlations to the explicit characteristics of the percolating rigid network. It demonstrates that (i) the pinchpoint appears only in an ensemble of

states where the rigid cluster has percolated, and ii) that the quantitative features of the pinchpoint is sensitive to whether the rigid cluster has percolated in one or both directions. Moreover, we have shown that the elastic moduli deduced from fitting the stress correlations to VCTG predictions is sensitive to normal stresses in the packing. This is completely expected in granular, jammed solids since they are created by normal stresses, but was not obvious for gels, which can be held together by interparticle forces, and prestresses exist even in the absence of externally applied stresses because of the inherent geometrical frustration that defines gels.

The success of VCTG in describing the elastic properties and the onset of rigidity in gels demonstrates the ubiquity of the constraints of mechanical equilibrium is shaping the properties of soft solids formed out of equilibrium. It also provides strong indication that the gauge-theoretic framework of VCTG is the correct approach to analyzing the stress response of such solids.

5 Recent Developments

In recent work [9], we have investigated the connection between the gauge potential φ_i and physical observables: although φ_i is not directly measurable due to gauge redundancy, spatial variations in φ_i relate to displacements caused by external forces, and can be measured in experiments. This establishes a direct link between the gauge theory and classical elasticity, with φ_i playing a role analogous to the displacement field u_i , albeit without reference to a unique stress-free configuration. Defining strain with respect to a reference configuration is thus akin to fixing a gauge within the VCTG framework. It is important to note that the physical dimensions of φ and \mathbf{u} differ, just at \hat{E} and the strain tensor $\hat{\gamma}$. VCTG predicts the Green’s function relating φ to an external force. For an isotropic elastic modulus tensor, the Green’s function depends on the shear modulus μ and the Poisson ratio, ν :

$$\varphi_i(\mathbf{q}) = -\mathcal{G}_{ij}^{-1}(\mathbf{q})f_j^{\text{ext}}(\mathbf{q}), \quad (22)$$

where,

$$\mathcal{G}_{ij}^{-1}(\mathbf{q}) = \frac{1}{g\mu q^2} \left(\delta_{ij} - \frac{1+\nu}{2} \frac{q_i q_j}{q^2} \right). \quad (23)$$

To relate φ to the displacement field \mathbf{u} , we have to introduce a proportionality constant $\beta(p)$ with dimensions of energy [9]:

$$u_i = \beta\varphi_i. \quad (24)$$

Here β encodes microscale information about the contact network. For isotropic, jammed packings it is a function of the pressure, and the scaling with pressure is determined by the nature of the soft-sphere interaction, harmonic or Hertzian [9].

In [9], we have also carefully analyzed evidence for any anomalies in the stress response and the displacement fields as one approaches the unjamming transition. In order to address this regime, we proposed a natural extension of the VCTG framework through gradient terms [52] and exploring the existence of an emergent length scale in

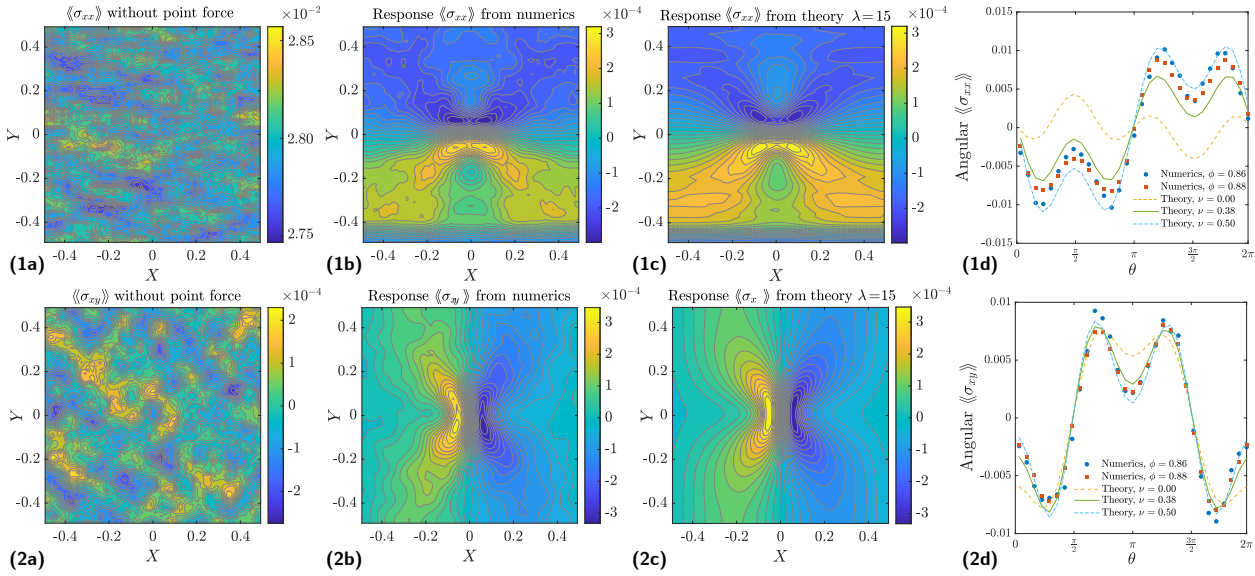


Figure 3. Comparisons between the theoretical predictions and numerical response to a point force in 2D [6] (Copyright (2022) by the American Physical Society). Rows (1) and (2) display the results for $\langle\langle\sigma_{xx}\rangle\rangle$ and $\langle\langle\sigma_{xy}\rangle\rangle$ respectively. The first column (a) displays the respective components of the background stress fluctuations. The second column (b) displays the response for each component of the stress tensor computed as a difference before and after the external forces are applied. The third column (c) displays the theoretical predictions for the response, computed for the simulation geometry using the Green’s function predicted by VCTG [6]. The fourth column (d) displays the quantitative comparison for the angular response from theory and numerics, obtained by integrating the response on an annulus of radius $r \in [0.075, 0.3]$ centered on the point force. The numerical results are given for two packing fractions $\phi = 0.85$ and 0.88 and the theoretical results are provided for three different Poisson’s ratio $\nu = 0.00, 0.38$ and 0.50 . The numerical results for the response of σ_{xx} have been symmetrized about the Y -axis as $\sigma_{xx}(x, y) = \frac{1}{2}(\sigma_{xx}(x, y) + \sigma_{xx}(-x, y))$ in order to reduce the noise in the data. The error bars in the angular response for σ_{xx}, σ_{xy} result from the background stress fluctuations in the packings.

the elastic response of jammed solids. This generalized theory incorporates both dielectric-like and Debye-type screening, distinguished by the magnitude of the screening length. If such a length scale exists, it should manifest in response functions. However, through numerical simulations of two-dimensional soft-sphere packings, we find no evidence of such a characteristic length scale in jammed solids. Instead, our results confirm that the dielectric response persists up to the jamming threshold [9]. Furthermore, studying grain displacement fields in response to localized perturbations, we find that variations in the φ field predict the structural patterns of grain displacements. Additionally, we unearthed the crucial role of disorder averaging in capturing the emergent elasticity of amorphous solids. Individual realizations can undergo irreversible rearrangements, leading to plastic responses. However, these plastic events do not persist upon ensemble averaging, indicating that their effects are statistical rather than defining a distinct pre-jammed phase. Although plasticity has been suggested to induce a finite screening length characteristic of a pre-jammed phase [28, 37], our numerical results show that the ensemble-averaged responses remain well described by dielectric VCTG screening. Specifically, we do not observe evidence of a pre-jammed phase characterized by a non-microscopic Debye-like screening length [9]. We do find evidence for the onset of nonlinear dielectric effects at very low pressures if the perturbing force is large compared to the contact forces. The VCTG dielectric formulation can certainly be generalized to in-

clude such nonlinearities by including a dependence of χ_{ijkl} on the perturbing forces. We are currently working on such a perturbative expansion.

The dynamical response of jammed solids, going beyond the electrostatic limit of VCT, can be mapped on to the full set of Maxwell’s equations. All of the equations, *except* the generalized Ampere’s law, involving the time derivative of stress, can be derived from Newton’s equations [6]. However, testing the applicability of the theory requires testing the postulated Ampere’s law mapping, and a precise definition of the \hat{B} field in terms of positions of grains. This work is now in progress.

6 Acknowledgements

This paper is based on the author’s collaborative work with Jishnu Nampoothiri, Michael D’Eon, Surajit Chakraborty, Albert Countryman, Kabir Ramola, H. Vinutha, Fabiola DeRuiz, Emanuela Del Gado and Xiaoming Mao. This work has been supported in part by the National Science Foundation grants: DMR-2026834 and CBET-2228681.

References

- [1] M.E. Cates, J.P. Wittmer, J.P. Bouchaud, P. Claudin, Phys. Rev. Lett. **81**, 1841 (1998)
- [2] L.D. Landau, L. Pitaevskii, A.M. Kosevich, E.M. Lifshitz, *Theory of elasticity: volume 7*, Vol. 7 (Elsevier, 2012)

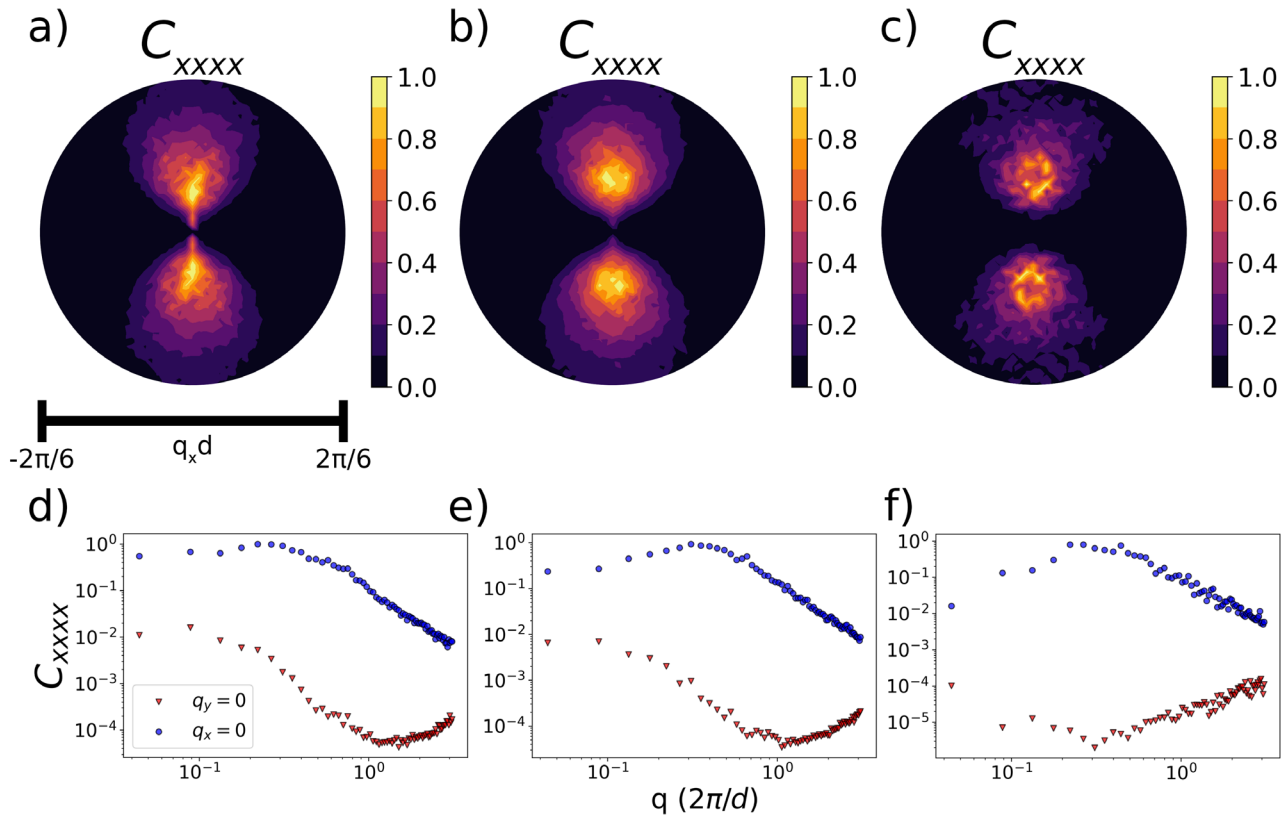


Figure 4. (Figure is taken from [52]) Analytical behavior of the pinch point singularity in $C_{ijkl}(\mathbf{q})$ correlates with degree of rigidity percolation [52]. Spectra of C_{xxxx} (normalized by the maximum value of C_{xxxx}) are ensemble averaged over configurations which exhibit rigidity percolation in 2 directions (a), 1 direction (b), and 0 directions (c). Cross sections of these spectra along $q_y = 0$ and $q_x = 0$ are shown in (d), (e), (f) in red and blue, respectively. The population of gels that did not percolate are shown to lack flat $|q|$ -dependence in $C_{ijkl}(\mathbf{q})$, indicating that these configurations are not rigid by the reckoning of VCTG.

- [3] J.P. Bouchaud, *Course 4: Granular Media: Some Ideas from Statistical Physics* (Springer Berlin Heidelberg, Berlin, Heidelberg, 2003), pp. 131–197, ISBN 9783540448358, https://doi.org/10.1007/978-3-540-44835-8_4
- [4] R.P. Behringer, B. Chakraborty, Reports on Progress in Physics **82**, 012601 (2019)
- [5] M. Pretko, Physical Review B **96**, 1 (2017), arXiv:1606.08857v1
- [6] J.N. Nampoothiri, M. D’Eon, K. Ramola, B. Chakraborty, S. Bhattacharjee, Physical Review E **106**, 065004 (2022)
- [7] J.N. Nampoothiri, Y. Wang, K. Ramola, J. Zhang, S. Bhattacharjee, B. Chakraborty, Physical review letters **125**, 118002 (2020)
- [8] H. Vinutha, F.D. Diaz Ruiz, X. Mao, B. Chakraborty, E. Del Gado, The Journal of chemical physics **158** (2023)
- [9] S. Chakraborty, J.N. Nampoothiri, S. Bhattacharjee, B. Chakraborty, K. Ramola, in Preparation
- [10] M. Cates, J. Wittmer, J.P. Bouchaud, P. Claudin, Physical review letters **81**, 1841 (1998)
- [11] A.J. Liu, S.R. Nagel, Nature **396**, 21 (1998)
- [12] D. Bi, J. Zhang, B. Chakraborty, R.P. Behringer, Nature **480**, 355 (2011)
- [13] V. Trappe, V. Prasad, L. Cipelletti, P. Segre, D.A. Weitz, Nature **411**, 772 (2001)
- [14] A. Gopal, D.J. Durian, Physical review letters **91**, 188303 (2003)
- [15] P. Chaudhuri, L. Berthier, W. Kob, Physical review letters **99**, 060604 (2007)
- [16] S. Zhang, E. Stanifer, V.V. Vasisht, L. Zhang, E. Del Gado, X. Mao, Physical Review Research **4**, 043181 (2022)
- [17] M. Otto, J.P. Bouchaud, P. Claudin, J.E.S. Socolar, Phys. Rev. E **67**, 031302 (2003)
- [18] A. Lemaître, J. Chem. Phys. **149**, 104107 (2018)
- [19] S. Gelin, H. Tanaka, A. Lemaître, Nature Materials **15**, 1177 (2016)
- [20] J. Geng, D. Howell, E. Longhi, R.P. Behringer, G. Reydellet, L. Vanel, E. Clément, S. Luding, Phys. Rev. Lett. **87**, 035506 (2001)
- [21] C.S. O’Hern, L.E. Silbert, A.J. Liu, S.R. Nagel, Phys. Rev. E **68**, 011306 (2003)
- [22] W. Ellenbroek, Ph.D. thesis, Leiden Institute of Physics, Institute-Lorentz for Theoretical Physics, Leiden University (2007), <https://scholarlypublications.universiteitleiden.nl/handle/1887/12083>

- [23] P.M. Chaikin, T.C. Lubensky, T.A. Witten, *Principles of condensed matter physics*, Vol. 10 (Cambridge university press Cambridge, 1995)
- [24] C.F. Schreck, T. Bertrand, C.S. O'Hern, M.D. Shattuck, *Phys. Rev. Lett.* **107**, 078301 (2011)
- [25] M.L. Falk, J. Langer, *Ann. Rev. Cond. Mat. Phys.* **2**, 353 (2011), 1004.4684
- [26] S. McNamara, J. Crassous, A. Amon, *Phys. Rev. E* **94**, 022907 (2016)
- [27] S. Karmakar, A. Lemaître, E. Lerner, I. Procaccia, *Phys. Rev. Lett.* **104**, 215502 (2010)
- [28] A. Lemaître, C. Mondal, M. Moshe, I. Procaccia, S. Roy, K. Sreiber-Réem, *Phys. Rev. E* **104**, 024904 (2021)
- [29] F. Radjai, D.E. Wolf, M. Jean, J.J. Moreau, *Physical review letters* **80**, 61 (1998)
- [30] Y. Jiang, H. Zheng, Z. Peng, L. Fu, S. Song, Q. Sun, M. Mayer, M. Liu, *Phys. Rev. E* **85**, 051304 (2012)
- [31] S. Luding, *International Journal of Solids and Structures* **41**, 5821 (2004)
- [32] A. Asaoka, *Soils and Foundations* **63**, 101294 (2023)
- [33] A.J. Liu, S.R. Nagel, W. van Saarloos, M. Wyart, *The jamming scenario - an introduction and outlook* (Oxford University Press, 2010), <https://oxford.universitypressscholarship.com/10.1093/acprof:oso/9780199691470.001.0001/acprof-9780199691470>
- [34] M. Pretko, *Phys. Rev. B* **96**, 125151 (2017)
- [35] N.S. Livne, A. Schiller, M. Moshe, *Phys Rev E* **107**, 055004 (2023)
- [36] A. Kumar, M. Moshe, I. Procaccia, M. Singh, *Phys Rev E* **106**, 015001 (2022)
- [37] Y. Fu, Y. Jin, D. Pan, I. Procaccia, arXiv preprint arXiv:2410.04138 (2024)
- [38] J.D. Jackson, *Classical electrodynamics*, 3rd edn. (Wiley, New York, NY, 1999), ISBN 9780471309321, <http://cdsweb.cern.ch/record/490457>
- [39] R. Artoni, A. Santomaso, P. Canu, *Phys. Rev. E* **79**, 031304 (2009)
- [40] Z. Shojaee, J.N. Roux, F.m.c. Chevoir, D.E. Wolf, *Phys. Rev. E* **86**, 011301 (2012)
- [41] M. Pretko, L. Radzihovsky, *Phys. Rev. Lett.* **120**, 195301 (2018)
- [42] S. Forest, Ecole des Mines de Paris, Paris pp. 1–20 (2005)
- [43] G. Lois, J. Zhang, T. Majmudar, S. Henkes, B. Chakraborty, C. O'Hern, R. Behringer, *Physical Review E* **80**, 060303 (2009)
- [44] A. Lemaître, *Physical Review E* **96**, 052101 (2017)
- [45] A. Lemaître, *The Journal of Chemical Physics* **149** (2018)
- [46] E. DeGiuli, *Physical review letters* **121**, 118001 (2018)
- [47] S. Henkes, B. Chakraborty, *Physical Review E* **79**, 061301 (2009)
- [48] S. McNamara, J. Crassous, A. Amon, *Physical Review E* **94**, 022907 (2016)
- [49] Y. Wang, Y. Wang, J. Zhang, *Nature communications* **11**, 4349 (2020)
- [50] T.S. Majmudar, R.P. Behringer, *Nature* **435**, 1079 (2005)
- [51] Y. Wang, Y. Wang, J. Zhang, *Nature Communications* **11**, 4349 (2020)
- [52] A. Countryman, H.A. Vinutha, F.D. Ruiz, X. Mao, E. Del Gado, B. Chakraborty, *Soft Matter* **21**, 4812 (2025)
- [53] R. Maharana, D. Das, P. Chaudhuri, K. Ramola, *Physical Review E* **109**, 044903 (2024)
- [54] R. Maharana, K. Ramola, *SciPost Physics* **17**, 012 (2024)
- [55] J.P. Snyder, *Map projections—A working manual*, Vol. 1395 (US Government Printing Office, 1987), <https://doi.org/10.3133/pp1395>
- [56] D. Bi, S. Henkes, K.E. Daniels, B. Chakraborty, *Ann. Rev. Cond. Mat. Phys.* **6**, 63 (2015)
- [57] S. Henkes, B. Chakraborty, *Phys. Rev. E* **79**, 061301 (2009)
- [58] E. De Giuli, *Phys. Rev. E* **101**, 043002 (2020), 1912.05970
- [59] G. Lois, J. Zhang, T.S. Majmudar, S. Henkes, B. Chakraborty, C.S. O'Hern, R.P. Behringer, *Phys. Rev. E* **80**, 060303(R) (2009)
- [60] R.P. Behringer, B. Chakraborty, *Reports on Progress in Physics* **82**, 012601 (2018)
- [61] S. Henkes, J. Schwarz, in *Statistical and Nonlinear Physics* (Springer, 2022), pp. 427–448
- [62] H.A. Vinutha, S. Sastry, *Physical Review E* **99**, 012123 (2019)
- [63] S. Zhang, L. Zhang, M. Bouzid, D.Z. Rocklin, E. Del Gado, X. Mao, *Physical review letters* **123**, 058001 (2019)
- [64] H. Tong, S. Sengupta, H. Tanaka, *Nature communications* **11**, 4863 (2020)